Quantum oscillations in a two-dimensional electron system under low-frequency microwave irradiation

Jian Mi,[1,2] Huiying Liu,[2] Junren Shi,[2,3] L. N. Pfeiffer,[4] K. W. West,[4] K. W. Baldwin,[4] and Chi Zhang[5,2,3,*]

[1]*Nanjing Research Institute of Electronic Technology, Nanjing 210039, China*

[2]*International Center for Quantum Materials, Peking University, Beijing 100871, China*

[3]*Collaborative Innovation Center of Quantum Matter, Beijing 100871, China*

[4]*Department of Electrical Engineering, Princeton University, Princeton, New Jersey 08544, USA*

[5]*SKLSM, Institute of Semiconductors, Chinese Academy of Science, P.O. Box 912, Beijing 100083, China*

(Received 23 August 2017; revised manuscript received 4 December 2019; published 19 December 2019)

We study the magnetoresistance of an ultrahigh mobility GaAs/AlGaAs two-dimensional electron system (2DES) in a weak magnetic field under low-frequency ($f < 20$ GHz) microwave (MW) irradiation. We observe that, with decreasing MW frequency, microwave induced resistance oscillations (MIRO) are damped and multiphoton processes become dominant. At very low MW frequency ($f < 4$ GHz), MIRO disappear gradually and an SdH-like oscillation develops. Our analysis indicates that the oscillation may originate from alternating Hall-field induced resistance oscillations (ac-HIRO), due to the transition from the elastic scattering in real space. On the other hand, from the view of photon energy, the oscillations can be understood as a multiphoton process of MIRO in the low MW frequency limit. We show that the two different nonequilibrium mechanisms of MIRO and HIRO can be unified under low-frequency MW irradiation.

DOI: 10.1103/PhysRevB.100.235437

The High quality GaAs/AlGaAs two-dimensional electron system (2DES) has been the optimal experimental platform for the study of the fractional quantum Hall effect (FQHE) for decades. Much attention has been paid to nonequilibrium transport properties of the 2DES at very high Landau levels (LLs); these properties include microwave induced resistance oscillations (MIRO) [1,2] and zero-resistance states (ZRS) [3,4], which can be expressed as a function of ω/ω_c, where $\omega = 2\pi f$ is the microwave (MW) frequency, $\omega_c = eB/m^*$ is the cyclotron frequency, and m^* is the effective mass of the electron. Another notable effect in 2DES is Hall field induced resistance oscillations (HIRO) or Zener tunneling that emerges in a dc electric field [5,6], which can be described as a function of $2R_c/\Delta Y$, where $2R_c$ is the cyclotron diameter, $\Delta Y = \hbar\omega_c/eE$ is the real space change due to the inter-Landau level spacing, and E is the Hall electric field.

Experimentally, MIRO and HIRO exhibit very similar features, but their physical origins are different. MIRO is understood in terms of MW induced impurity scattering (displacement model) [7] and a change of the distribution function (inelastic model) [8], while HIRO can be explained by inter-Landau-level elastic disorder, which relies on a large momentum transfer [5]. Experimental and theoretical efforts are made to explore the interaction between MIRO and HIRO [9–11]. It is found that the two oscillations mix nonlinearly when a 2DES is subject to microwave and a dc electric field simultaneously. The electron state transition can be viewed as either a jump in energy due to MW absorption or a jump in space due to elastic scattering from impurities under dc excitation [10]. From this point of view, HIRO and MIRO are considered as separate processes.

Most experiments about MIRO and ZRS are focused on high-frequency ($f > 30$ GHz) MW irradiation with high energy photon. The main limitation is that MW signals cannot be transmitted below the cutoff frequency within the rectangular waveguide. In this paper we expand the MW frequency range of MIRO by using a linear dipole antenna, and focus on the magnetoresistance oscillations under low-frequency ($f < 20$ GHz) MW irradiation. We observe abundant multiphoton processes of MIRO with decreasing MW frequency and a Shubnikov de–Haas (SdH)-like oscillation under low-frequency MW ($f < 4$ GHz).

The observation of SdH-like oscillations at low frequency MW irradiation is not new. It has been reported in experiments on a 2DES with mobilities of $\mu \sim 1 \times 10^6$ cm^2/V s at 4.2 K temperature [12–14]. Our study not only confirms the occurrence of SdH-like oscillations under low-frequency MW irradiation (cf. [15]), but also shows more oscillations and stronger oscillating features in ultrahigh mobility samples ($\mu \sim 3 \times 10^7$ cm^2/V s). With respect to the analysis, the oscillations are attributed to HIRO (or Zener tunneling) induced by MW irradiation [16]. In this paper we provide a different analysis.

We propose that the phenomenon can be accounted for by the multiphoton process of MIRO in the regime of frequency 100 MHz – 10 GHz. Given that the phenomenon in our observation is clear and strong, we perform a quantitative and analytic study by means of the quantum tunneling junction model [17]. Because the low-frequency MW irradiation is in

*gwlzhangchi@pku.edu.cn, zhangchi@semi.ac.cn

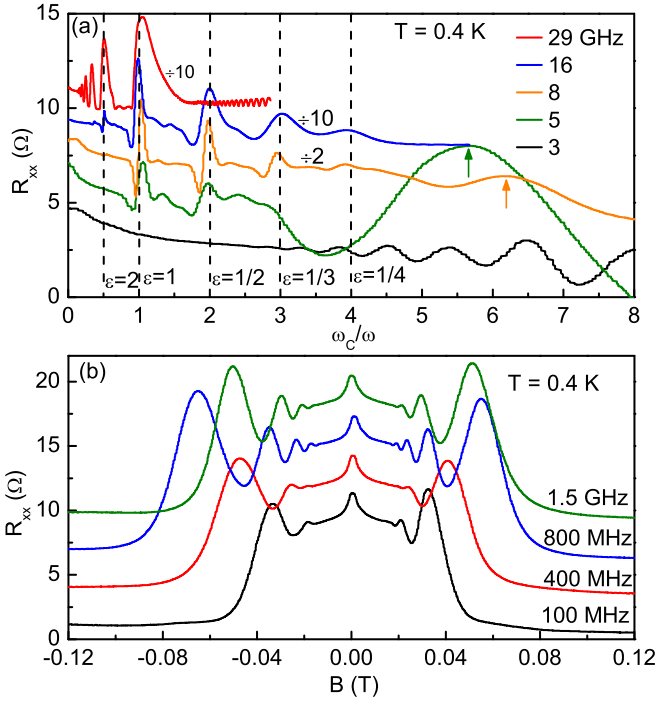

FIG. 1. (a) Magnetoresistances under MW irradiation from high frequency (29 GHz) to low frequency (3 GHz) are plotted against ω_c/ω, and the electron effective mass m^* is $0.067m_e$. The dashed lines indicate the multiphoton and harmonic process. (b) R_{xx} under-low frequency MW irradiation (<1.5 GHz). All the traces with vertical offset are shown for clarity.

the regime of multiphoton processes of MIRO [17] and, in addition, it satisfies the condition of HIRO [12–14], we interpret the oscillation by the equivalent effects of the multiphoton processes of MIRO and the ac-induced HIRO, whereby the two different nonequilibrium microscopic mechanisms could be unified under low-frequency MW irradiation. Thus the low-frequency MW induced oscillations supplement MIRO experiments.

Our experiments are carried out in a top-loading He-3 refrigerator with a base temperature of 0.3 K. A wafer with a high-quality ($\mu \sim 3 \times 10^7$ cm^2/V s) GaAs/$Al_{0.24}Ga_{0.76}$As quantum well (QW) is grown by molecular-beam epitaxy, and the carrier density is $n = 2.8 \times 10^{11}$ cm^{-2}. The 28-nm-wide QW is located about 320 nm beneath the sample surface. The Hall bar sample is defined by UV lithography and wet etching. Ohmic contacts are made by a 43/30/87 nm stack of Ge/Pd/Au metals with an annealing process at 450 °C. The microwave signal is generated by a continuous wave generator, Anritsu MG3690C, and is guided to the base via a semirigid coaxial cable, irradiating the sample by a linear dipole antenna hung over the sample. The distance between the antenna and the sample is about 1 cm. The MW frequency ranges from 8 MHz to 70 GHz. The resistance is measured by applying a low-frequency (17 Hz) external current $I =$ 100 nA through the Hall bar, and probing the voltage drop between two contacts.

Figure 1(a) illustrates the magnetoresistance under MW irradiation from 3 to 29 GHz. At $f = 29$ GHz, MIRO and ZRS are clearly observed. The major peaks are located near $\varepsilon = \omega/\omega_c = 1, 2, 3, \ldots$, which indicates that the harmonic

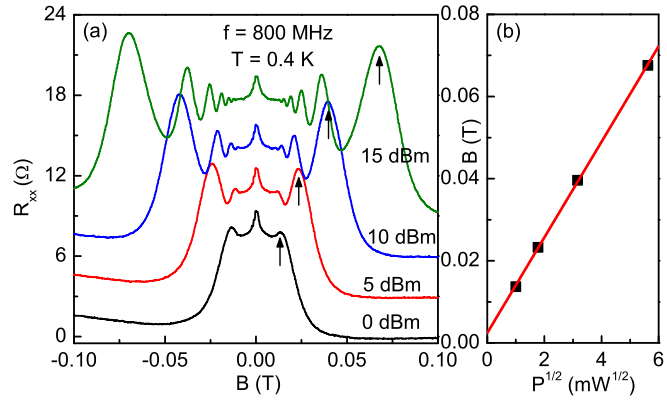

FIG. 2. (a) Power-dependent R_{xx} under 800 MHz microwave irradiation (with vertical offset for clarity). The upward arrows mark the largest resistance peaks of the oscillations. (b) The B positions of the marked peaks versus the square root of MW power (black squares). The red line is the linear fitting curve.

process is dominant: an electron absorbs one MW photon and jumps one or multiple LLs. However, with a lower frequency of $f = 16$ GHz, the resistance peaks below $\varepsilon = 2$ disappear, but peaks at $\varepsilon = 1/2, 1/3, 1/4$ develop; these are called multiphoton processes [18], in which an electron absorbs two or more MW photons and jumps one LL. Multiphoton processes only exist at low MW frequency ($f <$ 30 GHz). At $f = 8$ GHz, the peak at $\varepsilon = 2$ disappears, and the amplitude of MIRO decreases rapidly. Meanwhile, a small resistance peak near $\varepsilon = 1/6.2$ arises (marked by the orange color arrow), which cannot be explained by the regime of MIRO. The new peak (marked by the green color arrow) expands at $f = 5$ GHz, and grows stronger than MIRO. Finally, MIRO disappears completely at $f = 3$ GHz, and the new SdH-like oscillation becomes dominant. In general, with decreasing MW frequency and photon energy, MIRO decays gradually while the new oscillation emerges and develops. Figure 1(b) shows R_{xx} vs B under low MW frequency irradiation with $f = 1.5$ GHz, 800 MHz, 400 MHz, and 100 MHz. The new oscillations persist in a wide range of MW irradiation frequency. Like SdH oscillations, they are roughly $1/B$ periodic. And, similarly to MIRO and HIRO, the resistance oscillations are roughly symmetric with positive and negative magnetic fields, appearing only at very high LLs ($B < 0.1$ T).

The MW power-dependent results of the SdH-like oscillations for $f = 800$ MHz are shown in Fig. 2(a). The MW power values are obtained from the wave generator; the power loss in coaxial cables and the efficiency of the linear dipole antenna are not taken into account. The SdH-like oscillations are strongly dependent on MW power: at low power, the oscillations are weak and appear only at low magnetic fields. When the power increases, the oscillations extend to higher magnetic fields, and the number of peaks grows as well as the amplitudes of the oscillations. The B-field positions of the highest resistance peaks (marked by upward arrows) versus the square root of MW power are shown in Fig. 2(b). The linear relationship indicates that the B-field positions of the peaks are proportional to the electric component of the microwave [or electromagnetic (EM)] field. The f-dependent

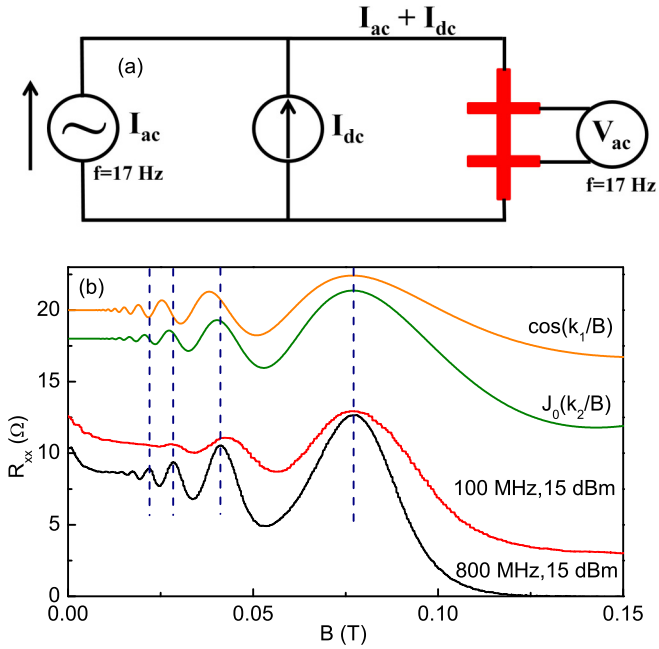

FIG. 3. (a) The diagram for the electrical measurement of HIRO. (b) The comparison of R_{xx} with cosine function and Bessel function. All traces are horizontally scaled to align with the largest oscillation peaks, and vertical offsets are provided for clarity. The dashed lines indicate the peaks of the 800 MHz trace.

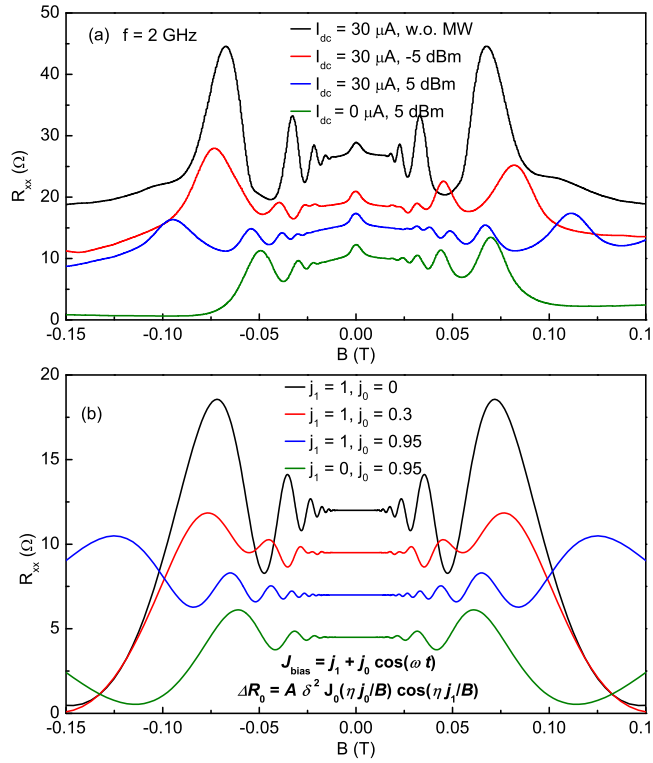

FIG. 4. (a) Magnetoresistance under MW irradiation for $f = 2$ GHz, with a dc-bias current passing through the Hall bar sample. The two kinds of oscillations merge into a new type of oscillation. (b) The traces of the formula $\Delta R_0 = A\delta^2 J_0(\eta \frac{j_0}{B}) \cos(\eta \frac{j_1}{B})$ are illustrated, where j_0 and j_1 are the relative amplitudes of the dc-bias and ac-bias current respectively. All the traces with vertical offset are shown for clarity.

oscillations in Fig. 1(b) originate from varying MW power at sample surface, because the attenuation of MW power is f dependent in the coaxial cable. The power-dependent features are different from MIRO, in which only the amplitudes change with MW power but the B-field positions remain constant. For HIRO, the oscillation is dependent on the dc-bias current density, akin to the SdH-like oscillations that are EM-field dependent. All these features suggest that the new oscillations may pertain to HIRO, which is consistent with the conclusion of previous experiments [12–14]. A more quantitative analysis is presented below.

Figure 3(a) displays a circuit diagram for the electrical measurement of HIRO. A constant dc current $I_{\rm dc}$ is applied through the Hall bar sample, along with a low frequency (17 Hz) modulation current $I_{\rm ac}$ of 100 nA. The voltage drop between the two contacts is recorded by a lock-in amplifier at the modulation frequency. The measured result is the differential magnetoresistance at a given dc bias: $r_{xx} = V_{\rm ac}/I_{\rm ac} = (\partial V/\partial I)_{\rm dc}$. When the 2DES sample is MW irradiated, an alternating current is excited in the Hall bar by the EM fields. The excited current plays the role of the bias current, causing the ac-HIRO effect.

For expository purposes, the magnetoresistance of dc-bias-induced HIRO can be described with a cosine function: $\Delta R = A\delta^2 \cos(\eta J_{\rm dc}/B)$ [5,6], where A is the amplitude, $\delta = \exp(-\pi/\omega_c \tau_q)$ is the Dingle factor from the SdH oscillations, τ_q is the quantum lifetime of electrons, and $J_{\rm dc}$ is the dc-bias current density. The factor can be expressed as $\eta = 4\pi m^* \sqrt{\frac{2\pi}{n}}/e^2$, in which n is the two-dimensional electron density. If the bias is an alternating current [16], $J_{\rm dc} = j_0 \cos(\omega t)$, where j_0 and ω are the amplitude and the frequency of the alternating current respectively. Thus ΔR changes with time rapidly. But in our measurement, the lock-in amplifier is locked at a low frequency of 17 Hz, and will only reach the zero frequency harmonic ΔR_0 from ΔR, because only ΔR_0 provides a term oscillating at 17 Hz. ΔR_0 is derived from Fourier transform:

$$\Delta R_0 = \frac{1}{T}\int_{-T/2}^{T/2} \Delta R\, dt = A\delta^2 J_0\left(\eta \frac{j_0}{B}\right). \qquad (1)$$

Therefore, the ac-HIRO result can be described as a simple Bessel function $J_0(x)$. The oscillation depends on the amplitude of the alternating current and the magnetic field, and j_0 is determined by the intensity of EM field or MW power, in accord with the power-dependent results in Fig. 2.

Figure 3(b) shows the comparison of R_{xx} under MW irradiation with cosine function and Bessel function. The traces of 100 and 800 MHz irradiation are both in line with the Bessel function trace, as opposed to the cosine function trace. The model of ac-HIRO accounts for the SdH-like oscillation.

To further demonstrate the close relationship between the SdH-like oscillation and HIRO, we study the magnetoresistance of the sample, which is subject to microwave irradiation and a dc-bias current simultaneously. The experimental results are shown in Fig. 4(a). Without MW irradiation, a strong dc-HIRO arises (shown by the black curve), which can be described as a cosine function. Meanwhile, with increasing

MW power, the oscillation expands to higher magnetic field and the amplitude decreases, as denoted by the red (−5 dBm) and the blue (5 dBm) traces. We find that the MW induced SdH-like oscillation (indicated by the green curve) and dc-induced HIRO (black curve) merge into a combined oscillation, which suggests that the mechanism of the SdH-like oscillation agrees with HIRO.

The calculation results of MW induced resistance oscillation are illustrated in Fig. 4(b). When the sample is driven by low-frequency MW irradiation and dc-bias current simultaneously, the bias can be expressed as a function of the driven frequency: $J_{\rm bias} = j_1 + j_0\cos(\omega t)$, where j_1 and j_0 are the amplitudes of the dc-bias current and the excited alternating current respectively. The zero-frequency harmonic is expressed as $\Delta R_0 = A\delta^2 J_0(\eta\frac{j_0}{B})\cos(\eta\frac{j_1}{B})$. The amplitudes of $j_1 = 1$ and 0 are consistent with the currents $I_{\rm dc} = 30\ \mu$A and 0 respectively, and $j_0 = 0.95$, 0.3, 0 correspond to the MW powers of 5 dBm, −5 dBm, and 0 (without MW irradiation). The difference in power of 10 dBm can be estimated from j_0: $20\log_{10}[\frac{j_{0,A}}{j_{0,B}}] = 20\log_{10}[\frac{0.95}{0.3}] = 20\log_{10}[3.1] = 10$ in dB.

The combined oscillation of dc-HIRO and ac-HIRO is determined by both j_1 and j_0. If the dc-bias current density j_1 is fixed, the MW irradiation can be viewed as a Bessel modulation on HIRO. Consequently, the B-field coordinate of the oscillation peaks increases with the MW power. The oscillating features from the calculations in Fig. 4(b) are very consistent with the observed experimental data in Fig. 4(a). This serves as strong quantitative evidence for the conclusion that the SdH-like oscillation originates from HIRO.

The MW signal in the ac-HIRO mechanism is considered as an excited bias current. We can also explain the oscillations in the view of microwave photons. Among the various theoretical models proposed for MIRO and ZRS, Shi and Xie put forward a quantum tunneling junction model [17], in which a periodic voltage $V_{\rm ac}$ (or electric field) can be induced by microwave (or rf) EM field. The obtained photon-assisted transport result of conductivity is derived as

$$\frac{\sigma}{\sigma_0} = \sum_{n=-\infty}^{\infty} J_n^2\left(\frac{\Delta}{\hbar\omega}\right)\left[1 + \frac{\lambda^2}{2}\cos\left(2\pi n\frac{\omega}{\omega_c}\right) - n\pi\lambda^2\frac{\omega}{\omega_c}\sin\left(2\pi n\frac{\omega}{\omega_c}\right)\right]. \quad (2)$$

σ and σ_0 are the conductances of the system with and without MW irradiation. The conductivity can be expressed as a function of MW power and frequency: Δ is the EM-field intensity, ω is the MW frequency, $\lambda = 2\exp(-\pi\omega_c\tau_q)$ is the Dingle factor, and $J_n(x)$ is the Bessel function of the nth order. The numerical results show that, with increasing MW power, the minimum of the conductance oscillation becomes negative and a zero resistance state emerges. When the power increases further, a multiphoton process sets in. Equation (2) can also be simplified as

$$\frac{\sigma}{\sigma_0} = 1 + \frac{\lambda^2}{2}J_0\left[\frac{2\Delta}{\hbar\omega}\sin\left(\frac{\pi\omega}{\omega_c}\right)\right] - \frac{\pi\lambda^2\Delta}{\hbar\omega_c}\cos\left(\frac{\pi\omega}{\omega_c}\right)J_1\left[\frac{2\Delta}{\hbar\omega}\sin\left(\frac{\pi\omega}{\omega_c}\right)\right].$$

At the low MW frequency limit ($\omega/\omega_c \to 0$), with $\sin(\frac{\pi\omega}{\omega_c}) \approx \frac{\pi\omega}{\omega_c}$ and $\cos(\frac{\pi\omega}{\omega_c}) \approx 1$, the change of conductance is

$$\frac{\Delta\sigma}{\sigma_0} = \frac{\lambda^2}{2}J_0\left(\frac{2\pi\Delta}{\hbar\omega_c}\right) - \frac{\pi\lambda^2\Delta}{\hbar\omega_c}J_1\left(\frac{2\pi\Delta}{\hbar\omega_c}\right) \approx \frac{\lambda^2}{2}J_0\left(\frac{2\pi\Delta}{\hbar\omega_c}\right) = \frac{\lambda^2}{2}J_0\left(\frac{2\pi m^*}{e\hbar}\frac{\Delta}{B}\right). \quad (3)$$

The result indicates that the conductance is not dependent on MW frequency, but depends on EM-field intensity at the low-frequency limit. The quantum tunneling junction model provides an explanation: under low MW frequency irradiation with low photon energy, an electron absorbs multiple photons and jumps one LL. The new oscillation can be regarded as a multiphoton process of MIRO at the low MW frequency limit. Equation (3) on the low-frequency limit of MIRO has the same form as Eq. (1) on the HIRO phenomenon, where $\lambda = 2\delta$, and Δ corresponds to j_0. We explain the new oscillations with either the multiphoton process of MIRO or ac-HIRO, under the condition of the low MW frequency limit. MIRO describes electron transitions from the photon absorption in energy, while HIRO depicts the transition from the elastic scattering in space. Low-frequency MW irradiation is in between the two limits of bias for MIRO (high-frequency MW) and HIRO (dc-bias). These two mechanisms can be integrated into one under low-frequency MW irradiation.

In summary, in our ultrahigh mobility n-type GaAs/AlGaAs quantum well, we expand the MW frequency range of MIRO and focus on magnetoresistance oscillations under low-frequency (<20 GHz) MW irradiation. We find that, with decreasing frequency, multiphoton assisted MIRO is observed, and when MIRO disappears gradually a SdH-like oscillation develops. The SdH-like oscillation is dependent on MW power rather than MW frequency. We provide a quantitative analysis of the phenomenon in terms of the multiphoton process of MIRO at the low MW frequency limit. Moreover, we prove the equivalence of the bias current induced ac-HIRO and the multiphoton process of MIRO in the low-frequency regime. Thus the two different nonequilibrium mechanisms of MIRO and HIRO can be unified under low-frequency MW irradiation. It is a desirable approach to perceive the two mechanisms in a unified theory. Our findings contribute to the understanding of the relationship between MIRO and HIRO.

This project is supported by the National Science Foundation of China (Grants No. 11674006 and No. 11974339) and National Basic Research Program of China (Grant No. 2014CB920904). The work at Princeton University is funded by the Gordon and Betty Moore Foundation through the EPiQS initiative Grant GBMF4420, and by the National Science Foundation MRSEC Grant DMR-1420541. J.M. and C.Z. performed the experiments; H.L. and J.S. provided the theoretical discussions; J.M. and C.Z. analyzed the data and wrote the paper; L.N.P., K.W.W. and K.W.B. grew the semiconductor wafers; C.Z. conceived and supervised the project.

[1] M. A. Zudov, R. R. Du, J. A. Simmons, and J. L. Reno, Phys. Rev. B **64**, 201311(R) (2001).
[2] P. D. Ye, L. W. Engel, D. C. Tsui, J. A. Simmons, J. R. Wendt, G. A. Vawter, and J. L. Reno, Appl. Phys. Lett. **79**, 2193 (2001).
[3] R. G. Mani, J. H. Smet, K. von Klitzing, V. Narayanamurti, W. B. Johnson, and V. Umansky, Nature (London) **420**, 646 (2002).
[4] M. A. Zudov, R. R. Du, L. N. Pfeiffer, and K. W. West, Phys. Rev. Lett. **90**, 046807 (2003).
[5] C. L. Yang, J. Zhang, R. R. Du, J. A. Simmons, and J. L. Reno, Phys. Rev. Lett. **89**, 076801 (2002).
[6] W. Zhang, H.-S. Chiang, M. A. Zudov, L. N. Pfeiffer, and K. W. West, Phys. Rev. B **75**, 041304(R) (2007).
[7] Adam C. Durst, Subir Sachdev, N. Read, and S. M. Girvin, Phys. Rev. Lett. **91**, 086803 (2003).
[8] I. A. Dmitriev, M. G. Vavilov, I. L. Aleiner, A. D. Mirlin, and D. G. Polyakov, Phys. Rev. B **71**, 115316 (2005).
[9] A. T. Hatke, H.-S. Chiang, M. A. Zudov, L. N. Pfeiffer, and K. W. West, Phys. Rev. B **77**, 201304(R) (2008).
[10] W. Zhang, M. A. Zudov, L. N. Pfeiffer, and K. W. West, Phys. Rev. Lett. **98**, 106804 (2007).
[11] A. T. Hatke, H.-S. Chiang, M. A. Zudov, L. N. Pfeiffer, and K. W. West, Phys. Rev. Lett. **101**, 246811 (2008).
[12] A. A. Bykov, A. K. Bakarov, A. K. Kalagin, and A. I. Toropov, JETP Lett. **81**, 284 (2005).
[13] A. A. Bykov, A. K. Bakarov, A. K. Kalagin, A. V. Goran, A. I. Toropov, and S. A. Vitkalov, Physica E **34**, 97 (2006).
[14] A. A. Bykov, A. V. Goran, D. R. Islamov, A. K. Bakarov, J.-q. Zhang, and S. Vitkalov, arXiv:cond-mat/0603398.
[15] R. L. Willett, L. N. Pfeiffer, and K. W. West, Phys. Rev. Lett. **93**, 026804 (2004).
[16] A. A. Bykov, J. Q. Zhang, Sergey Vitkalov, A. K. Kalagin, and A. K. Bakarov, Phys. Rev. B **72**, 245307 (2005).
[17] Junren Shi and X. C. Xie, Phys. Rev. Lett. **91**, 086801 (2003).
[18] M. A. Zudov, R. R. Du, L. N. Pfeiffer, and K. W. West, Phys. Rev. B **73**, 041303(R) (2006).